Measurements of Warm Dark Matter Properties

Bruce Hoeneisen

Universidad San Francisco de Quito, Quito, Ecuador

Reunion Island, 9 November, 2022

Warm dark matter observables

The adiabatic invariant:

$$v_{h\mathrm{rms}}(1) \equiv v_{h\mathrm{rms}}(a)a = v_{h\mathrm{rms}}(a)\left[\frac{\Omega_c \rho_{\mathrm{crit}}}{\rho_h(a)}\right]^{1/3},$$

At t_{eq}, the free-streaming power spectrum cut-off factor is

$$\tau^2(k) \approx \exp\left(-k^2/k_{\mathrm{fs}}^2(t_{\mathrm{eq}})\right), \qquad k_{\mathrm{fs}}(t_{\mathrm{eq}}) = \frac{1.455}{\sqrt{2}}\sqrt{\frac{4\pi G\bar{\rho}_m(1)a_{\mathrm{eq}}}{v_{h\mathrm{rms}}(1)^2}}.$$

Challenge: Measure the adiabatic invariant $v_{h\mathrm{rms}}(1)$, the comoving free-streaming cut-off wavenumber $k_{\mathrm{fs}}(t_{\mathrm{eq}})$, and the velocity dispersion linear perturbation cut-off mass M_{vd}, and check their consistency.

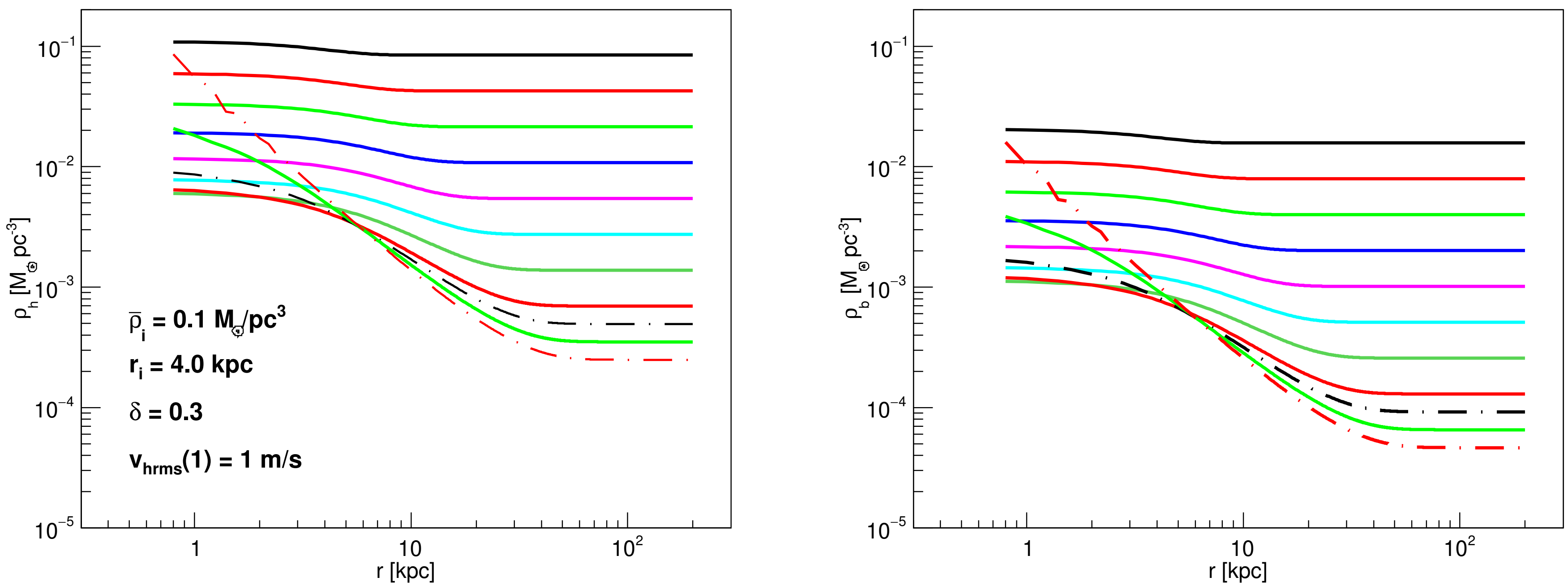

Shown are the cold dark matter and baryon densities as a function of r and t during the formation of a galaxy.

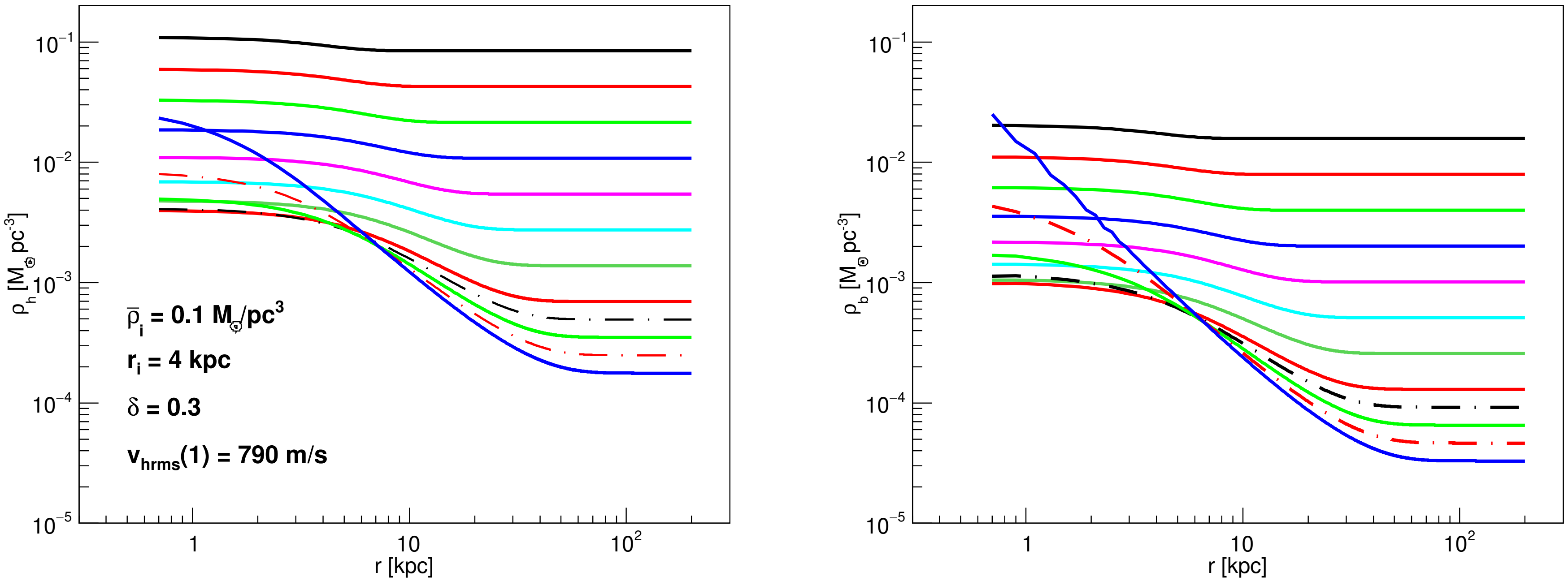

Shown are the warm dark matter and baryon densities as a function of r and t during the formation of an elliptical galaxy. Note: DM core, delayed formation, $\rho_b(0) > \rho_h(0) \rightarrow$ stars, $v_{h\mathrm{rms}}(1)$.

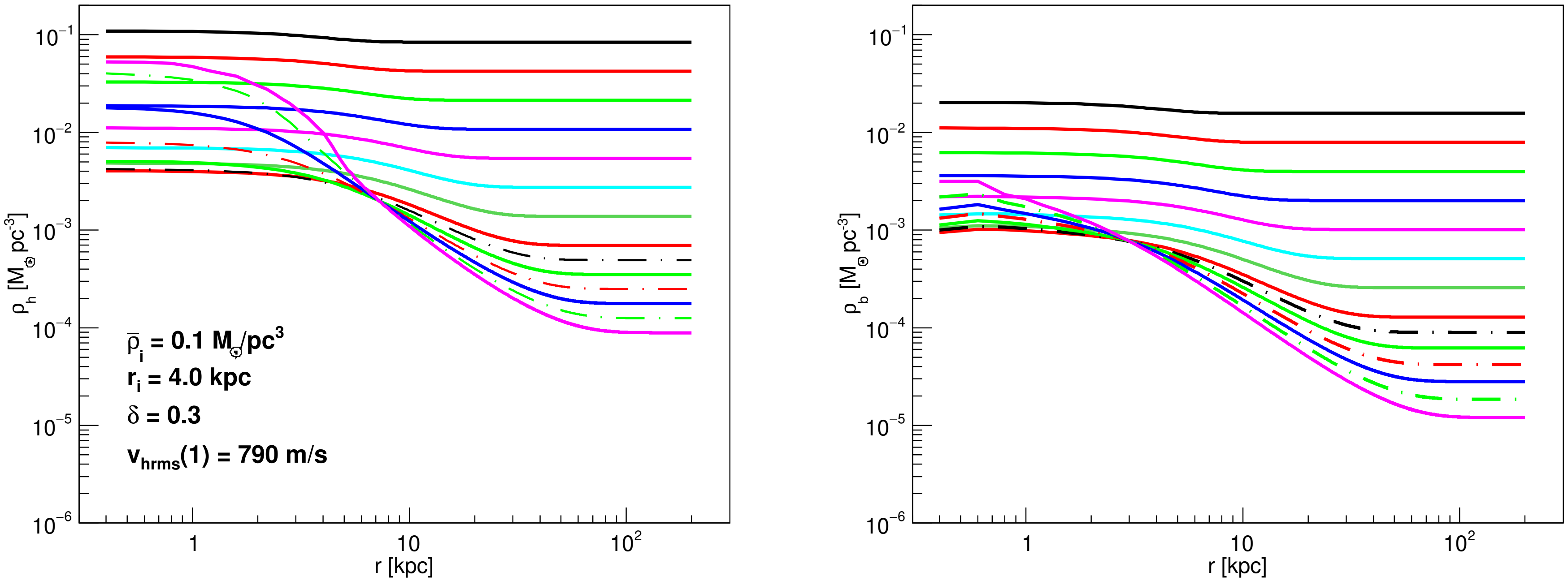

Shown are the warm dark matter and baryon densities as a function of r and t during the formation of a spiral galaxy with angular momentum.

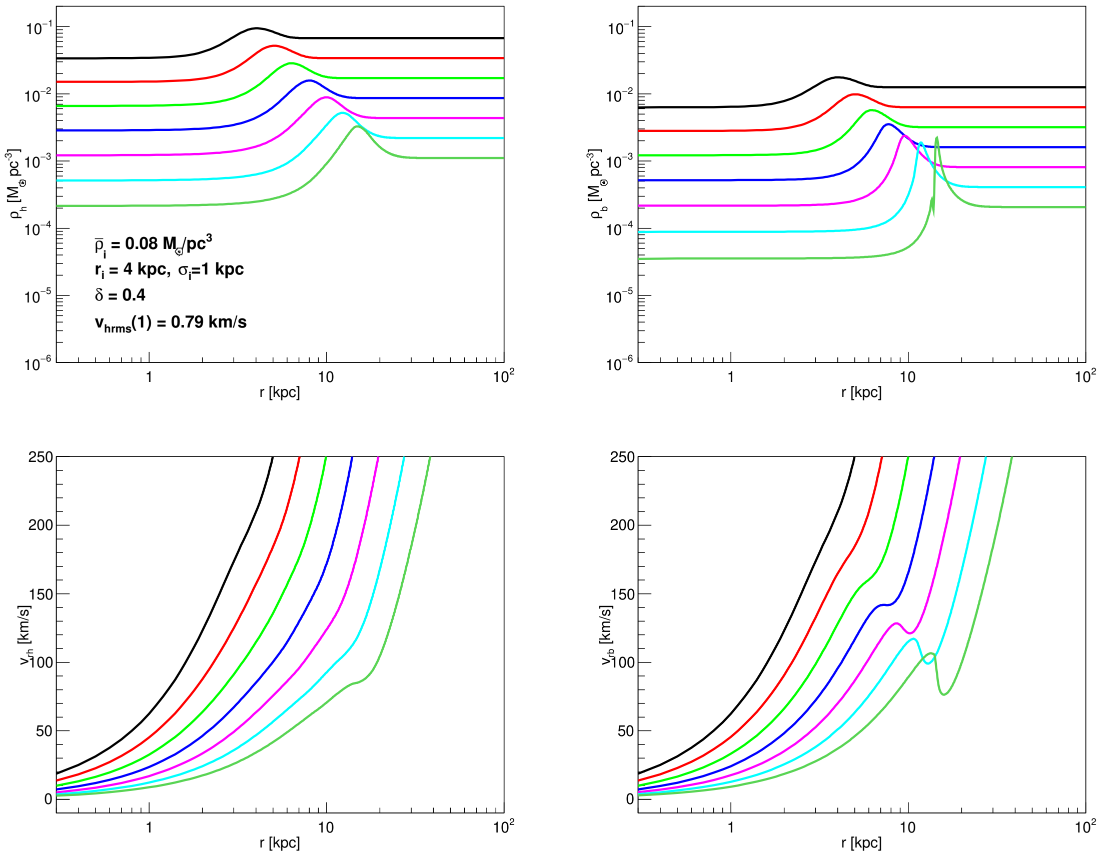

Shown are the warm dark matter and baryon densities and velocities as a function of r and t during the formation of a spherical sheet.

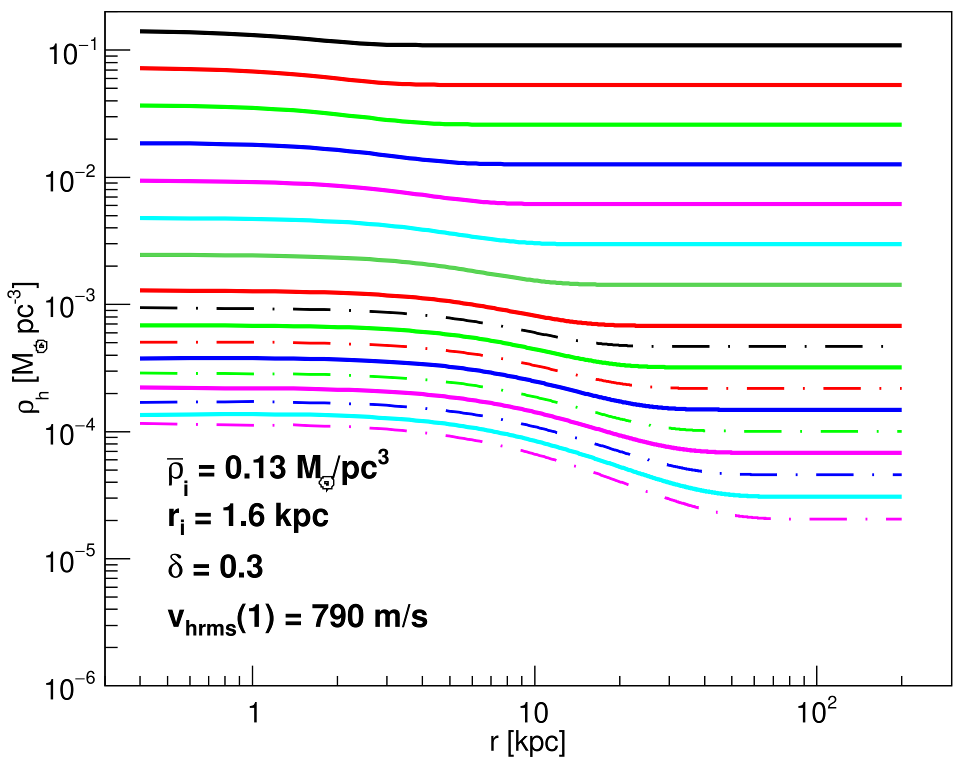

If the linear mass $M = M_h + M_b$ is below the velocity dispersion cut-off M_{vd}, formation of a gravitationally bound structure is delayed or absent.

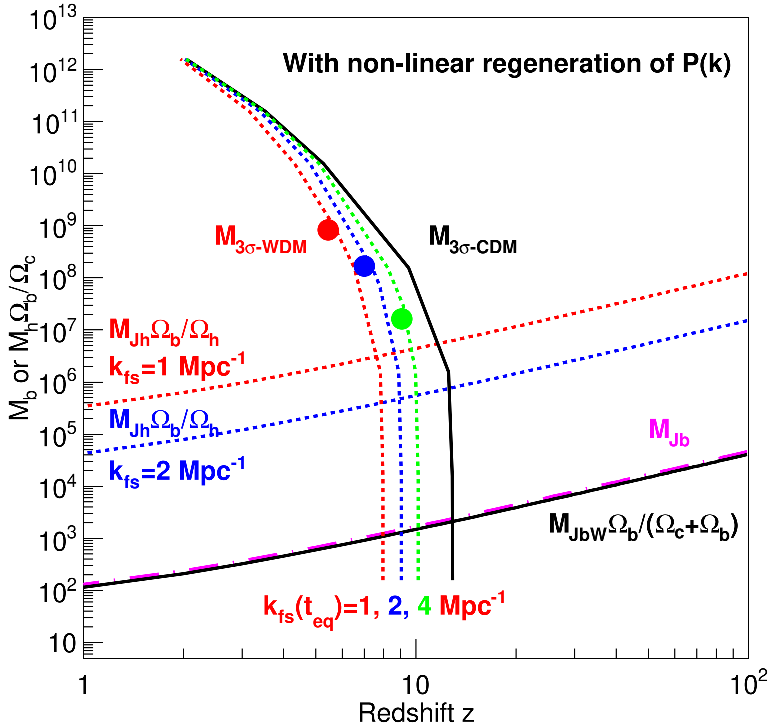

Contours of $1.686 = 3\sigma(M, k_{\rm fs}, z)$ illustrate formation of “first” galaxies. Valid only above the velocity dispersion cut-offs indicated by dots. Note that 2 Mpc^{-1} $\lesssim k_{\rm fs} \lesssim$ 4 Mpc^{-1}. Three observables of ΛWDM: $v_{h\rm rms}(1)$, $k_{\rm fs}(t_{\rm eq})$, $M_{\rm vd}$.

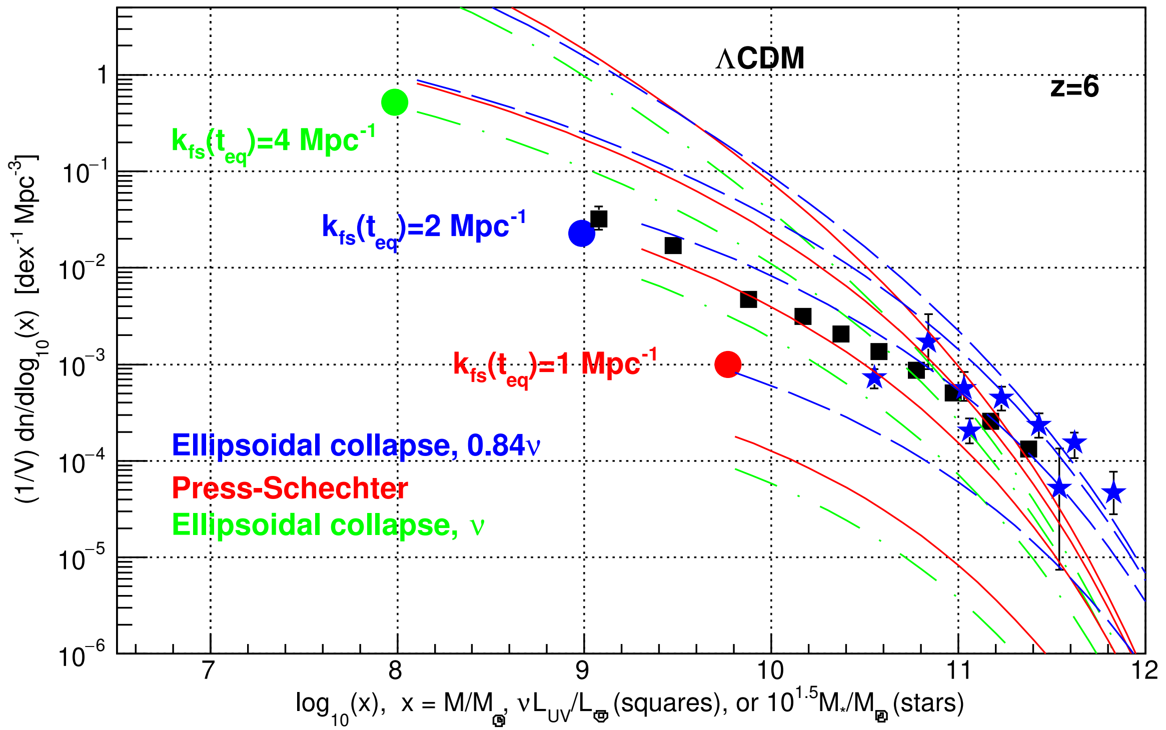

Shown are distributions of predicted linear masses $M/M_\odot$ (lines), observed stellar masses $10^{1.5} M_*/M_\odot$ (blue stars), and rest frame ultra-violet luminosities $\nu L_{\mathrm{UV}}/L_\odot$ (black squares), at redshift $z = 6$. Note that $k_{\mathrm{fs}} \approx 2$ Mpc^{-1}.

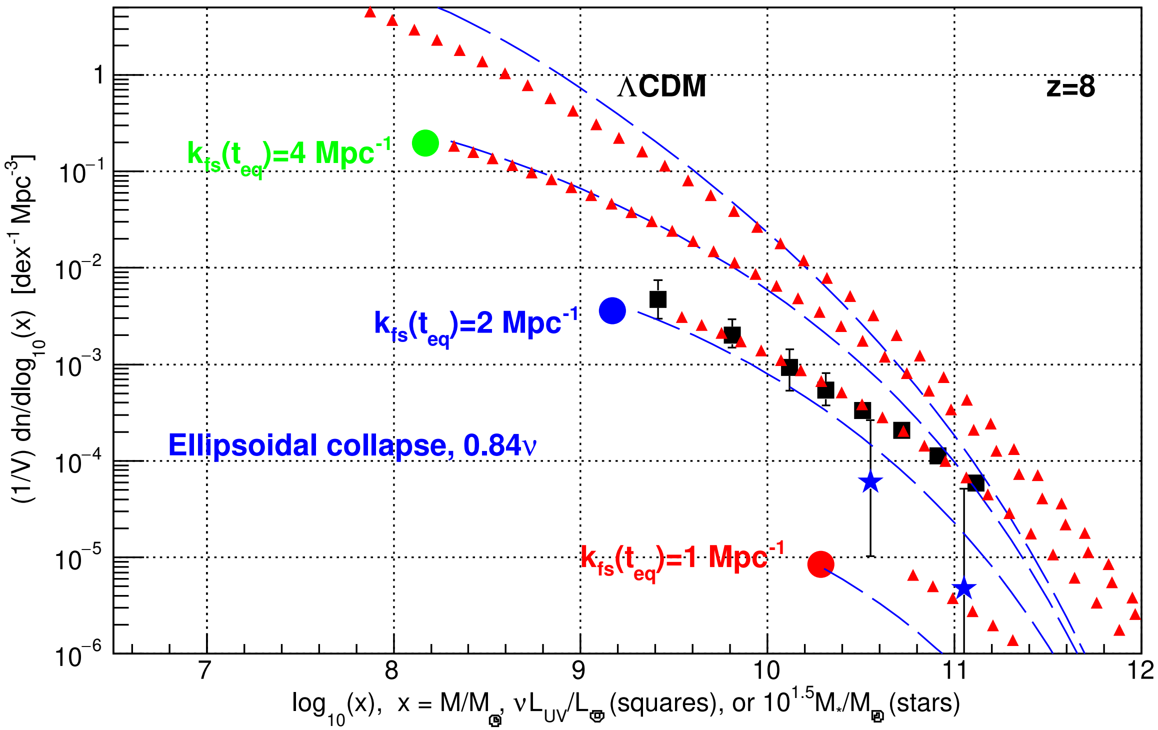

Shown are distributions of predicted linear masses $M/M_\odot$ (lines), UV luminosities (red triangles), observed stellar masses $10^{1.5} M_*/M_\odot$ (blue stars), and rest frame ultra-violet luminosities $\nu L_{\text{UV}}/L_\odot$ (black squares), at redshift $z = 8$. Note that $k_{\text{fs}} \approx 2$ Mpc^{-1}.

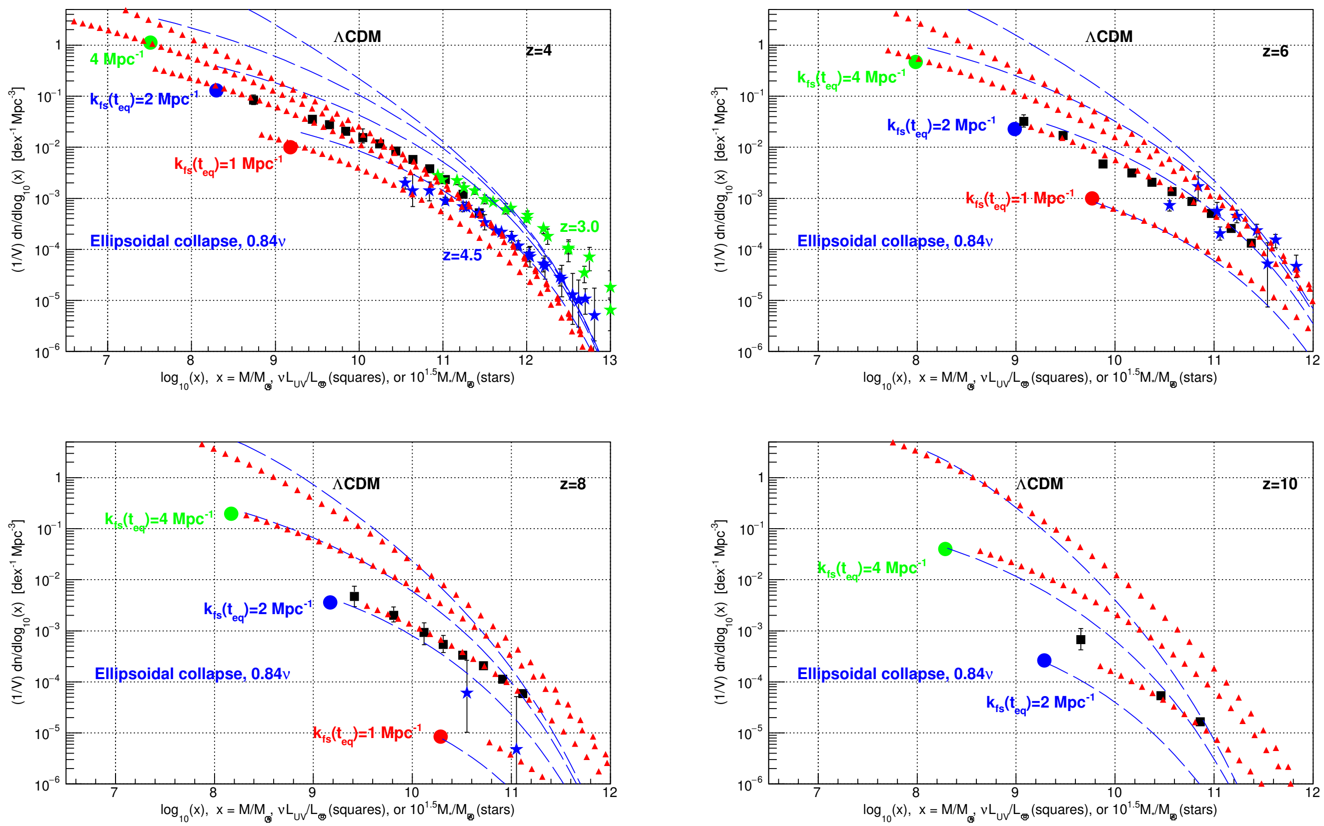

Same for $z = 4, 6, 8, 10$. Note that $k_{\mathrm{fs}} \approx 2\ \mathrm{Mpc}^{-1}$.

At $z = 8$, for each $k_{\mathrm{fs}}(t_{\mathrm{eq}})$ are presented the velocity dispersion cut-off $M_{\mathrm{vd}}/M_{\odot}$ of the linear total (dark matter plus baryon) mass $M/M_{\odot} \approx \nu L_{\mathrm{UV}}/L_{\odot}$, the corresponding cut-off AB-magnitude M_{UV}, and the reionization optical depth τ. The Planck collaboration obtains $\tau = 0.054 \pm 0.007$. Note that $k_{\mathrm{fs}} \approx 2$ Mpc^{-1}.

$k_{\mathrm{fs}}(t_{\mathrm{eq}})$	$M_{\mathrm{vd}}/M_{\odot}$	M_{UV} cut-off	τ
1 Mpc^{-1}	2×10^{10}	-19.9	0.047 ± 0.006
2 Mpc^{-1}	1.5×10^{9}	-17.0	0.053 ± 0.006
4 Mpc^{-1}	1.5×10^{8}	-14.5	0.060 ± 0.008

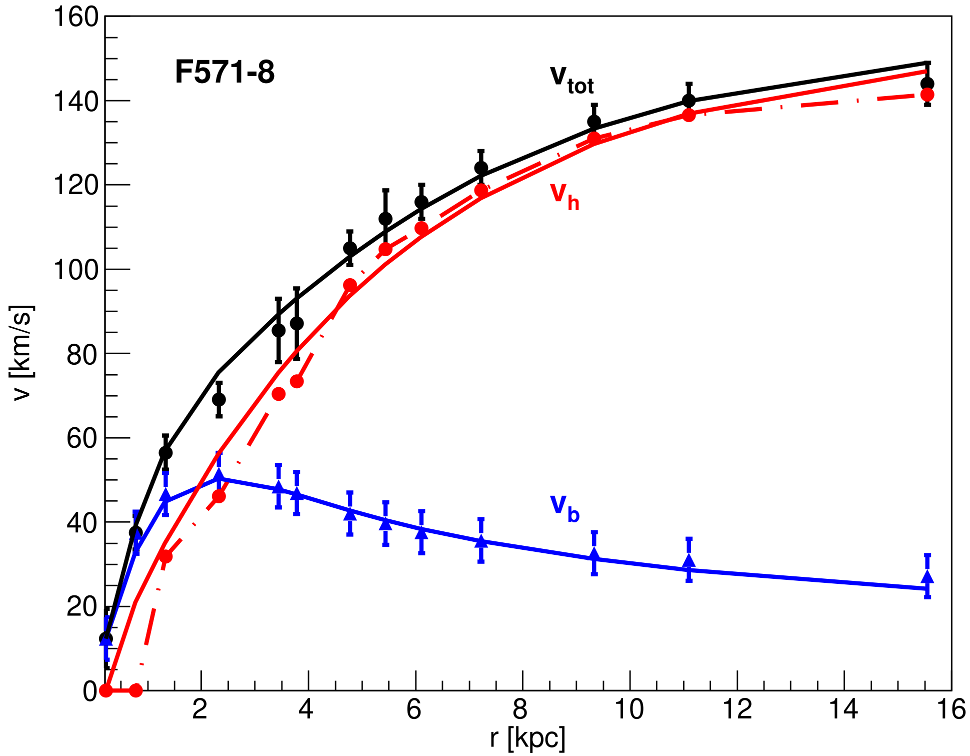

Rotation curves of spiral galaxy F571-8 (in SPARC sample), compared to numerical calculation that obtains $\rho_h(r \to 0)$, $\langle v_{rh}^2 \rangle$, $\rho_b(r \to 0)$, and $\langle v_{rb}^2 \rangle$.

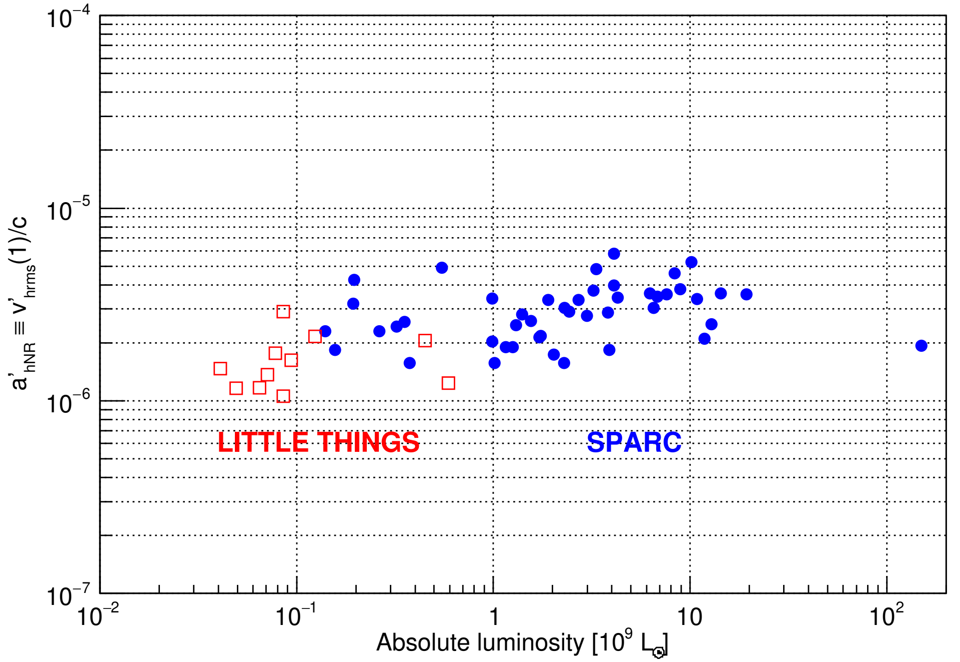

The expansion parameter at which dark matter becomes non-relativistic (uncorrected for dark matter rotation and relaxation) $a'_{h\text{NR}} \equiv v'_{h\text{rms}}(1)/c$, as a function of the absolute luminosity, of 11 LITTLE THINGS dwarf galaxies, and 46 spiral galaxies in the SPARC sample.

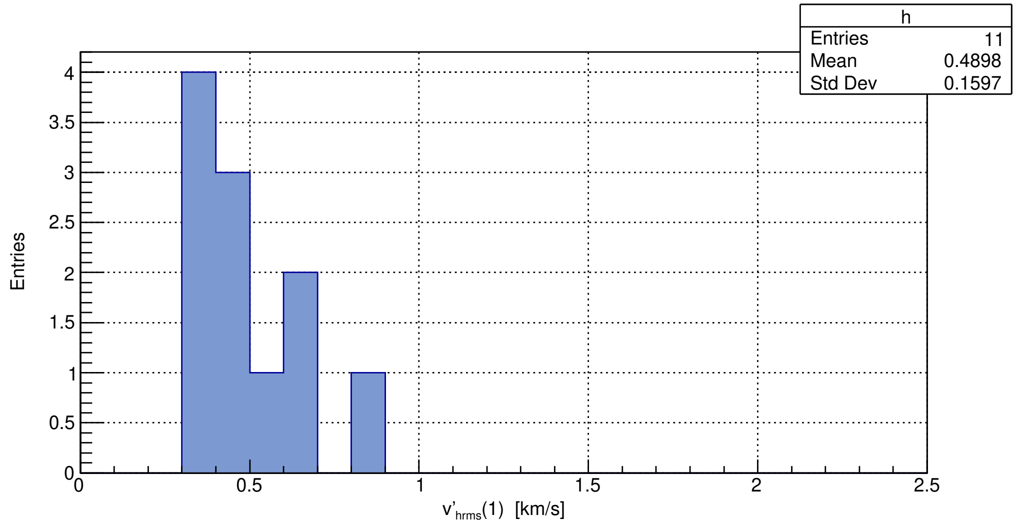

Distribution of the adiabatic invariant $v_{h\text{rms}}(1)$, uncorrected for rotation and relaxation, of 11 dwarf galaxies outside of the Milky Way. Peak corresponds to $k_{\text{fs}} \approx 2\ \text{Mpc}^{-1}$.

Measurements of the adiabatic invariant $v_{h\text{rms}}(1)$ with 56 spiral galaxy rotation curves, the comoving free-streaming cut-off wavenumber $k_{\text{fs}}(t_{\text{eq}})$ with galaxy stellar mass distributions at $z = 4.5, 6, 7$ and 8, and galaxy UV luminosity distributions at $z = 4, 6, 8$ and 10, reionization, first galaxies, M_{vd}, 11 dwarf galaxies, and predictions from the no freeze-in and no freeze-out scenario. $a'_{h\text{NR}} \equiv v_{h\text{rms}}(1)/c$. After e^+e^- annihilation $0.424 \geq T_h/T \geq \mathbf{0.344}$, or $T_C < T_{\text{dec}} < \mathbf{m_t}$.

Observable	$v_{h\text{rms}}(1)$ [km/s]	$10^6 a'_{h\text{NR}}$	$k_{\text{fs}}(t_{\text{eq}})$ [Mpc^{-1}]	m_h [eV]
Spiral galaxies	0.79 ± 0.33	2.64 ± 1.10	$1.03^{+0.74}_{-0.30}$	
M_* distribution	$0.91^{+0.72}_{-0.30}$	$3.02^{+2.42}_{-0.99}$	$0.90^{+0.44}_{-0.40}$	
First galaxies	≈ 0.4 to 0.2	≈ 1.4 to 0.7	≈ 2 to 4	
M_* and L_{UV}	$0.41^{+0.14}_{-0.12}$	$1.36^{+0.45}_{-0.39}$	$2.0^{+0.8}_{-0.5}$	
Reionization	≈ 1.2 to 0.2	≈ 3.9 to 0.5	≈ 0.7 to 5.4	
Vel. disp. cut-off	< 0.54	< 1.8	> 1.5	
Dwarf galaxies	0.41 ± 0.07	1.35 ± 0.23	$2.01^{+0.41}_{-0.29}$	
Fermions spin 1/2 **				
No freeze-in/-out	1.93 to **0.83**	6.43 to **2.78**	0.42 to **0.98**	54 to **101**
Bosons				
No fr-in/-out spin 0	1.12 to **0.48**	3.73 to **1.61**	0.73 to **1.69**	81 to **152**
No fr-in/-out spin 1 *	2.24 to **0.97**	7.46 to **3.22**	0.36 to **0.84**	40 to **76**

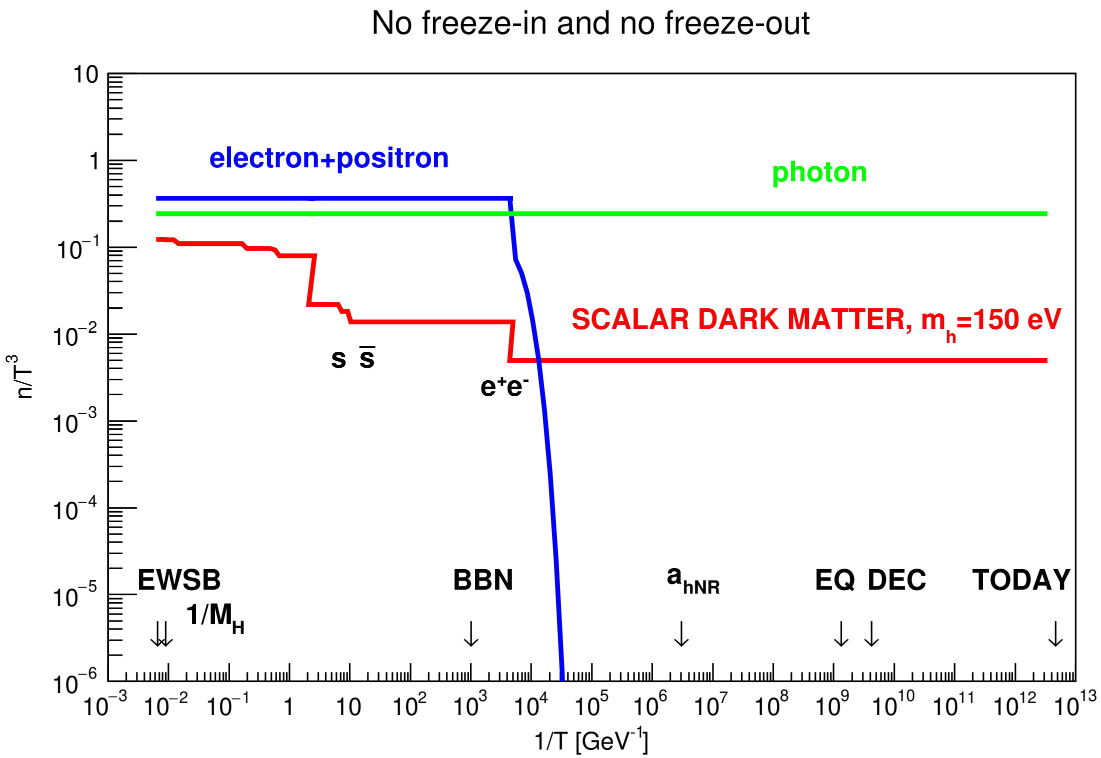

The no freeze-in and no freeze-out warm dark matter scenario is illustrated with an example. T is the photon temperature, and the n's are particle number densities.

For full details of this short talk, and for the sources of all data shown, see

- Hoeneisen, B. (2019) A Study of Dark Matter with Spiral Galaxy Rotation Curves. *International Journal of Astronomy and Astrophysics*, **9**, 71-96.
- Hoeneisen, B. (2019) The adiabatic invariant of dark matter in spiral galaxies. *International Journal of Astronomy and Astrophysics*, **9**, 355-367.
- Hoeneisen, B. (2022) Comments on Warm Dark Matter Measurements and Limits *International Journal of Astronomy and Astrophysics*, **12**, 94-109.
- +9
- Hoeneisen, B. (2022) Measurement of the Dark Matter Velocity Dispersion with Galaxy Stellar Masses, UV Luminosities, and Reionization *International Journal of Astronomy and Astrophysics*, **12**, 258-272.

and references therein.

Conclusions

- We have independently and redundantly obtained each of three observables (the adiabatic invariant $v_{h\text{rms}}(1)$, the free-streaming cut-off wavenumber $k_{\text{fs}}(t_{\text{eq}})$, and the velocity dispersion cut-off mass M_{vd}), from DATA. The data are spiral galaxy rotation curves, first galaxies, the distributions of galaxy stellar masses M_* and rest frame UV luminosities L_{UV}, reionization and dwarf galaxies. These measured observables turn out to be consistent with each other. They determine the temperature-to-mass ratio of dark matter, not separately temperature $T_h(a)$ or mass m_h.

- This measured temperature-to-mass ratio happens to be consistent with the no freeze-in and no freeze-out scenario for spin

0 warm dark matter that decouples early on from the standard model sector.

- One example is scalar dark matter S, that couples to the Higgs boson ϕ, and has a mass $m_h = 150 \pm 2$ eV. $\mathcal{L} = \mathcal{L}_{\mathrm{SM}} + \frac{1}{2}\partial_\mu S \cdot \partial^\mu S - \frac{1}{2}\bar{m}_S^2 S^2 - \frac{\lambda_S}{4!} S^4 - \frac{1}{2}\lambda_{hS}\left(\phi^\dagger \phi\right) S^2$.

- According to "The Review of Particle Physics" (2022), limits on dark matter particle mass are $m_h > 70$ eV for fermions, and $m_h > 10^{-22}$ eV for bosons. May I suggest that limits on the "thermal relic mass" of order keV that can be found in the literature, which are in disagreement with the measurements presented above, be revised with the inclusion of the non-linear regeneration of small scale structure, and the velocity dispersion cut-off.

Questions?

Summary of measurements and predictions. After e^+e^- annihilation, while dark matter is ultra-relativistic, $0.424 \geq T_h/T \geq \mathbf{0.344}$, corresponding to decoupling at $T_C < T_{\text{dec}} < \mathbf{m_t}$.

Observable	$v_{h\text{rms}}(1)$ [km/s]	$10^6 a'_{h\text{NR}}$	$k_{\text{fs}}(t_{\text{eq}})$ [Mpc^{-1}]	m_h [eV]
Spiral galaxies	0.79 ± 0.33	2.64 ± 1.10	$1.03^{+0.74}_{-0.30}$	
M_* distribution	$0.91^{+0.72}_{-0.30}$	$3.02^{+2.42}_{-0.99}$	$0.90^{+0.44}_{-0.40}$	
First galaxies	≈ 0.4 to 0.2	≈ 1.4 to 0.7	≈ 2 to 4	
M_* and L_{UV}	$0.41^{+0.14}_{-0.12}$	$1.36^{+0.45}_{-0.39}$	$2.0^{+0.8}_{-0.5}$	
Reionization	≈ 1.2 to 0.2	≈ 3.9 to 0.5	≈ 0.7 to 5.4	
Vel. disp. cut-off	< 0.54	< 1.8	> 1.5	
Dwarf galaxies	0.41 ± 0.07	1.35 ± 0.23	$2.01^{+0.41}_{-0.29}$	
Fermions spin 1/2 **				
No freeze-in/-out	1.93 to **0.83**	6.43 to **2.78**	0.42 to **0.98**	54 to **101**
Bosons				
No fr-in/-out spin 0	1.12 to **0.48**	3.73 to **1.61**	0.73 to **1.69**	81 to **152**
No fr-in/-out spin 1 *	2.24 to **0.97**	7.46 to **3.22**	0.36 to **0.84**	40 to **76**

Backup Slides

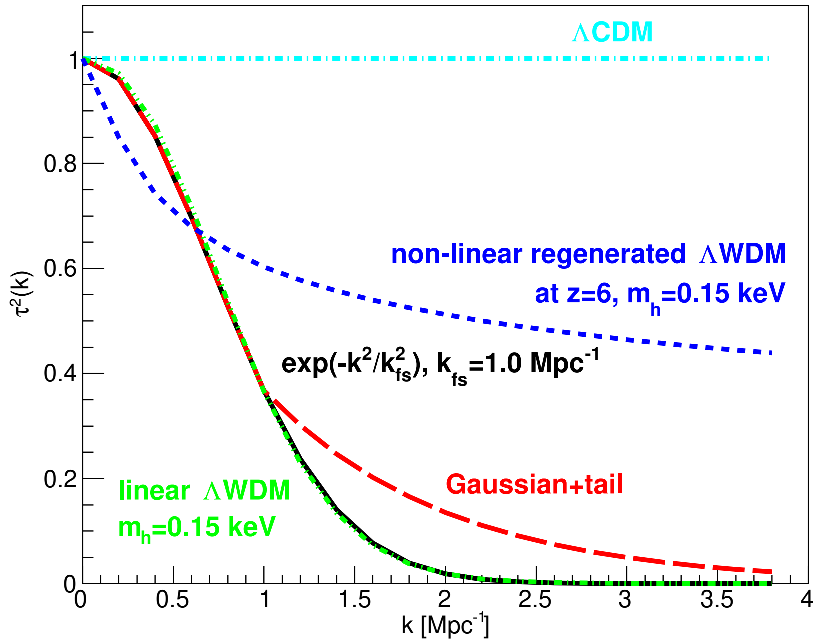

Power spectrum free-streaming cut-off factor $\tau^2(k)$ without, and with, non-linear regeneration of small scale structure.

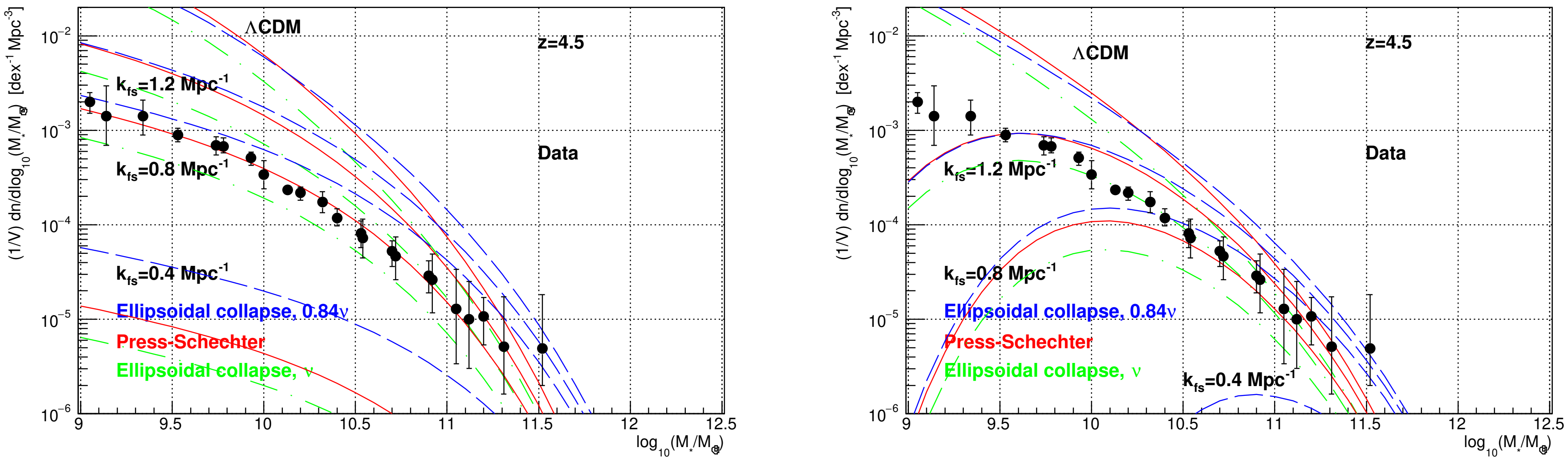

Comparison of data with the Press-Schechter predictions for Gaussian and sharp-k window functions assuming no non-linear regeneration of small scale structure.

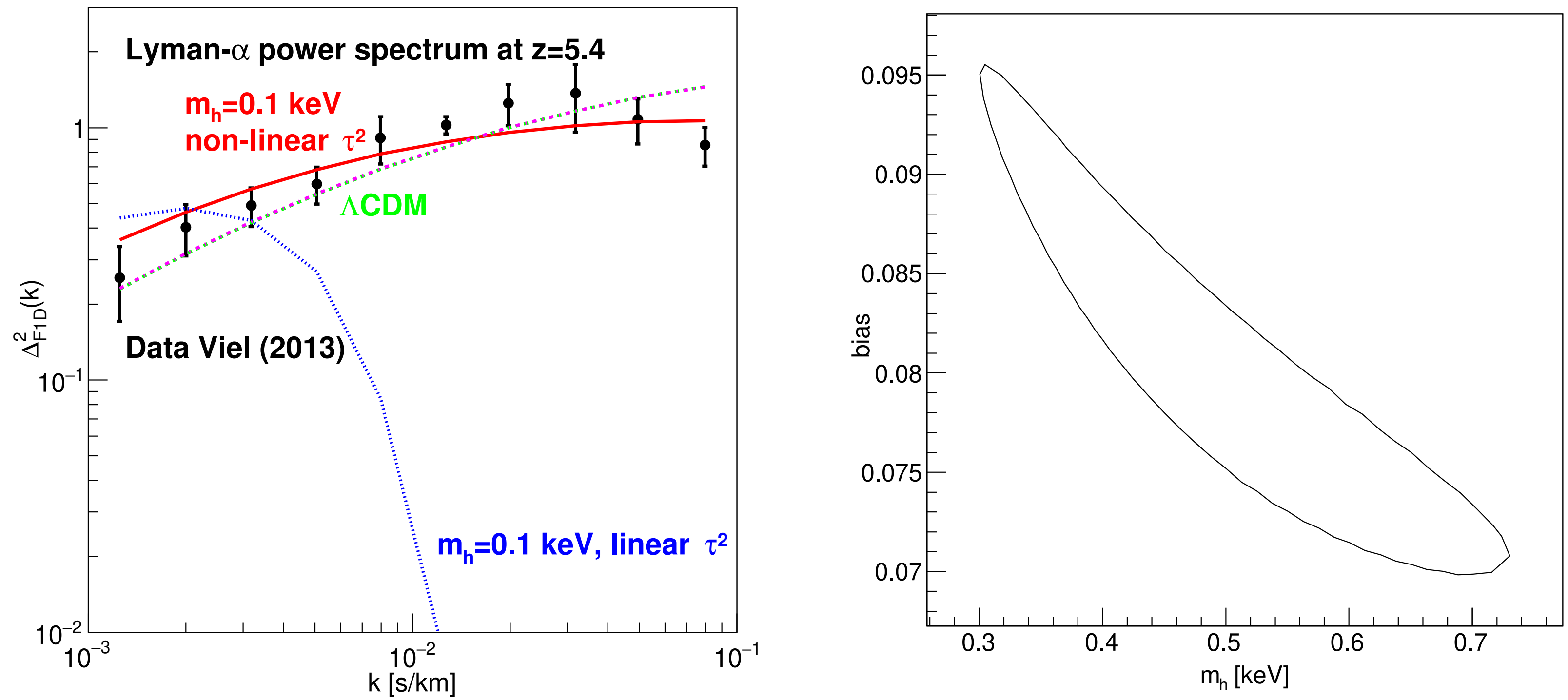

Measured Lyman-α 1D power spectrum at $z = 5.4$, compared with predictions of ΛCDM, and ΛWDM with the free-streaming cut-off factor $\tau(k)$ without, and with, a non-linear re-generated "tail".

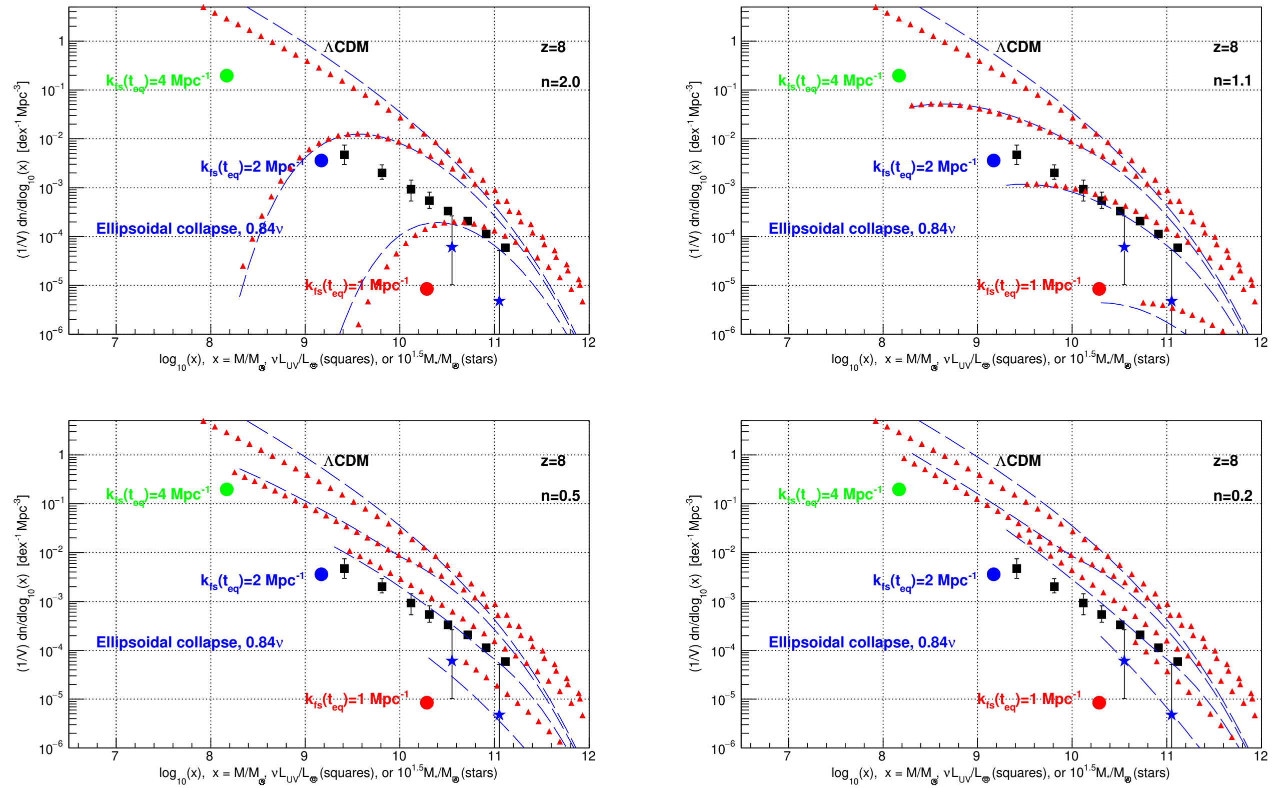

$\tau^2(k) = \exp\left(-k^2/k_{\text{fs}}^2(t_{\text{eq}})\right)$ if $k < k_{\text{fs}}(t_{\text{eq}})$, else $= \exp\left(-k^n/k_{\text{fs}}^n(t_{\text{eq}})\right)$ with $n = 2.0, 1.1, 0.5,$ or 0.2. The window function is sharp-k. $n = 2$ corresponds to no non-linear regenerated tail.

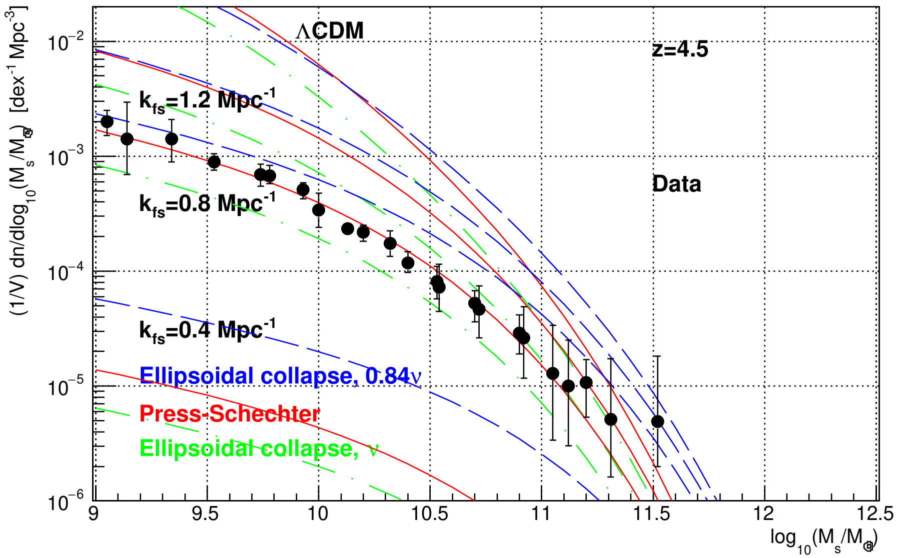

Calculated stellar mass functions with the Press-Schechter, Ellipsoidal Collapse with $\tilde{\nu} = \nu$, and Ellipsoidal Collapse with $\tilde{\nu} = 0.84\nu$ approximations, for ΛCDM, and ΛWDM with $k_{\rm fs} = 1.2, 0.8$ and 0.4 $\rm Mpc^{-1}$, at redshift $z = 4.5$, compared with observations.

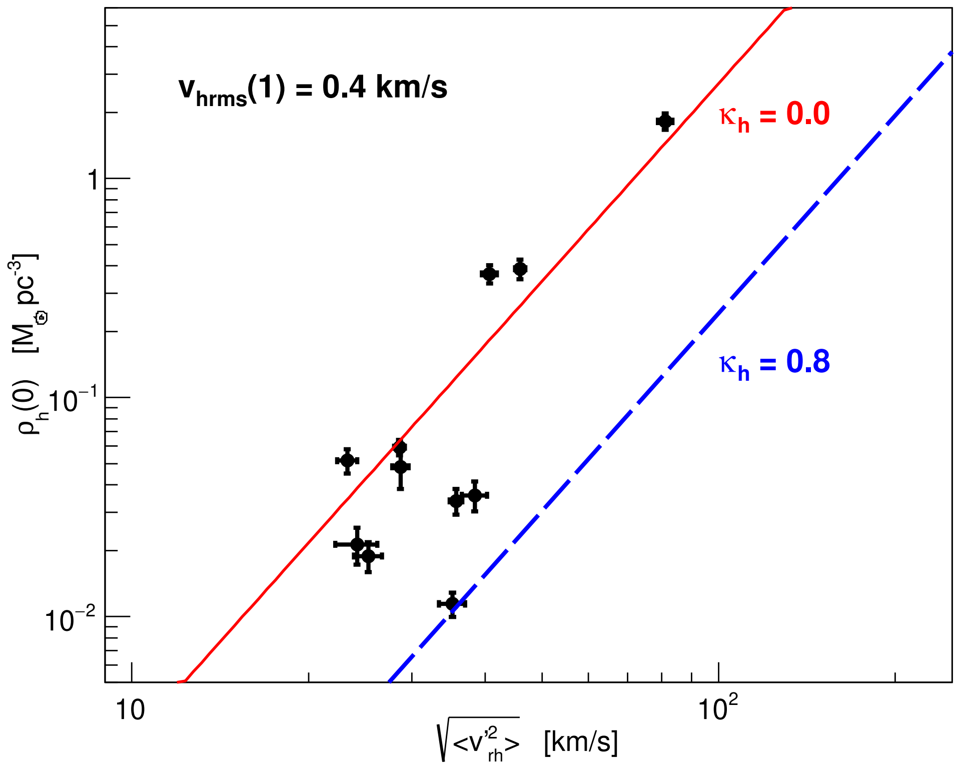

Shown are $\sqrt{\langle v'^2_{rh} \rangle}$ vs. $\rho_h(0)$, of 11 LITTLE THINGS galaxies, with statistical uncertainties only. Dark matter halo rotation and relaxation increse $v'_{h\text{rms}}(1)$.